ICM11

Assessment of Debonding-Induced Toughening in Nanocomposites

M. Zappalorto*, M. Salviato, M. Quaresimin

University of Padova, Department of Management and Engineering, Str. San Nicola 3, Vicenza 36100, Italy

Abstract

The high mechanical performances achievable by nanomodification of polymeric resins at low nanofiller volume fractions are related to the energy dissipated through the damage mechanisms taking place at the nanoscale. Among the others, nanoparticle debonding could take an important role either as a mechanism itself or as a trigger for mechanisms like plastic void growth or matrix shear yielding. In the present work, a model for the assessment of the extension and the shape of the debonding region (DBR) and the toughness improvement due to nanoparticle debonding is presented. The model takes into account some important issues inherently related to the nanoscale with particular reference to the emergence of an interphase surrounding the nanoparticle. Results can be useful in the scope of a multi-scale modelling strategy to the problem.

Keywords: polymer nanocomposites; nanoparticles; multiscale modelling; debonding; debonding region (DBR); interphase.

1. Introduction

The understanding of the relation between the nanostructure and the overall mechanical behaviour of nanocomposites plays an important role in the development of such new class of materials. This need has given rise in the literature to a large number of heterogeneous modelling strategies.

Discrete computational modelling techniques, such as Molecular Dynamics (MD), have been recently employed to investigate nanocomposite systems [1-4] as well as Nanostructural models, which account for the influence of morphology and nanostructure, but not for the molecular interactions. Among the strategies employing nanostructural models, worth of mentioning are the works by Thostenson and Chou [5], who proposed a modelling strategy for epoxy matrix reinforced by aligned MWCNTs, and by Luo and Daniel [6] who studied the prediction of elastic properties of PLS nanocomposites, accounting for the

* Corresponding author. *E-mail address*: zappalorto@gest.unipd.it

nanoclay morphology, the actual nanofiller orientation and grade of exfoliation.

Representative studies on the reinforcing influence exerted by nanoparticles on the mechanical properties of epoxy resins have been carried out by Wetzel *et al.* [7] and Zhao *et al.* [8]. The nanoparticle size effect on the energy dissipation due to the interfacial debonding has been studied by Chen *et al.* [9], who derived a simple size-dependent formulation for the debonding stress, which was later used to compute the energy dissipation due to interfacial debonding.

Lauke [10] analysed the energy dissipation phenomena by considering, besides particle debonding, voiding and subsequent yielding of the polymer, while Williams [11] analysed in detail the toughening of particle filled polymers due to plastic void growth around debonded or cavitated particles.

More recently the present authors explicitly considered the effect of the interphase zone surrounding the nanoparticle on the debonding stress [12]; such a zone, due to inter and supra-molecular interactions, might be characterised by chemical and physical properties different from those of the constituents [1, 2]. The aim of the study was to determine a closed form expression for the critical debonding stress accounting for the properties of an interphase zone between the nanoparticle and the matrix.

Starting from this previous work, in the present paper we present a multiscale model with the aim to determine:

-   the extension and the shape of the Debonding Region (DBR), namely the region of material around the crack tip interested by nanoparticle debonding as well as the number of nanoparticles subjected to debonding within the DBR;
-   the toughness improvement due to nanoparticle debonding.

2. Description of the multiscale system under analysis

Within the frame of a hierarchical multiscale model, the analysis has to be carried out at different length scales. Each of these can be addressed separately, inputs being provided by the solution of the previous model (at the smaller scale).

Starting from the macroscale, we initially consider a crack in the nano-modified matrix (see Fig. 1). The hydrostatic stress component of the crack tip stress fields under plane strain conditions turns out to be:

$$\sigma_h = \frac{\sigma_x + \sigma_y + \sigma_z}{3} = \frac{2(1+\nu_o)K_I}{3\sqrt{2\pi\rho}}\cos\frac{\phi}{2} \qquad (1)$$

where K_I and ν_o are the Irwin stress intensity factor and the Poisson coefficient of the nanocomposite, respectively.

Different from traditional micro-reinforced composites, in nanostructured materials the surface effect becomes significant and might have a substantial influence on the overall properties [13]. On the other hand, the data available so far in the literature about the interphase zone are not enough to formulate precisely the law of variation of its properties across the thickness, as well as its size, those parameter varying from case to case. Then, according to [12], in the present work we adopt the simplified hypothesis that the through-the-thickness averaged properties are representative of the overall property distribution within the interphase, which is also assumed as homogeneous and isotropic.

The required properties and size of the interphase can be computed by means of some analyses carried out within the frame of Molecular Dynamics as done in [1, 2]. Thus the system under investigation at the nanoscale, shown in Fig. 1, is constituted by a spherical nanoparticle of radius $\mathbf{r_0}$, a shell-shaped interphase of external radius **a** and uniform properties, and matrix of radius **b** much greater than $\mathbf{r_0}$ and **a**, and subjected to a uniform hydrostatic stress.

The crack-induced macroscale stress, σ_h, can be thought of as the average of microscale stresses over a Representative Volume Element (RVE). By using the *Average-Stress Theorem* and the Mori-Tanaka approximation this mean value can be linked to the hydrostatic stress component around the nanoparticle [14]:

$$\sigma_n(\rho, \phi) = \frac{\sigma_h}{C_h} = \frac{1}{C_h} \frac{2(1 + \nu_o) K_I}{3\sqrt{2\pi\rho}} \cos\frac{\phi}{2} \tag{2}$$

where C_h is reciprocal of the hydrostatic part of the global stress concentration factor, and can be determined as:

$$C_h = \frac{K_m}{K_p} \times \zeta \tag{3}$$

ζ being known in closed form [12], and K_m and K_p being the matrix and nanoparticle bulk moduli, respectively.
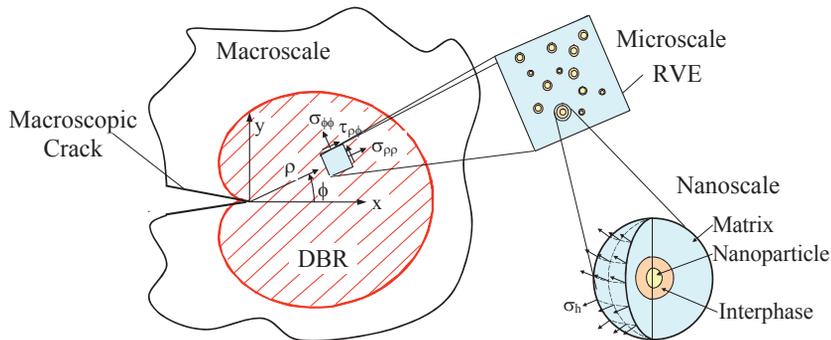
Fig. 1. Description of the multiscale system under analysis.

3. Assessment of the debonding region (DBR)

The extension of the debonding region, meant as the region around the crack tip containing all the nanoparticles where debonding damage is expected to occur, can be assessed by equating σ_n with the critical debonding stress σ_{cr}:

$$\sigma_{cr} = \sigma_n(\rho, \phi) = \frac{1}{C_h} \times \frac{2(1 + \nu_o) K_I}{3\sqrt{2\pi\rho}} \cos\frac{\phi}{2} \tag{4}$$

where σ_{cr} can be determined according to the following equation [12]:

$$\sigma_{cr} \cong \sqrt{\frac{4\gamma}{r_0} \times \frac{E_m}{1 + \nu_m}} \times \left[1 + \left(\beta \times \sqrt{\frac{E_a}{E_m} \times \frac{1 + \nu_m}{1 + \nu_a}} - 1 \right) \times \left(1 - e^{\left[\left(1 - \frac{a}{r_0} \right) \times \frac{10}{3} \right]} \right) \right] \tag{5}$$

Further details on Eq. (5) can be found in [12]. Note that the simplified failure criterion used in Eq. (4) might be improved by including a statistical distribution of the interfacial strength, according to [9]. Solving Eq. (4) by ρ results in:

$$\rho^*(\phi) = \frac{1}{(C_h)^2} \times \frac{2(1+\nu_o)^2 K_I^2}{9\pi\sigma_{cr}^2} \cos^2\left(\frac{\phi}{2}\right) = A \times \cos^2\left(\frac{\phi}{2}\right) \tag{6}$$

A schematic representation of the debonding region (DBR) is also depicted in Fig. 1.

The number of nanoparticles subjected to debonding, N_p, and the total surface subjected to debonding, S_p, can then be determined as:

$$N_p = \int_V \frac{f_{p0}}{4/3\pi r_0^3} dV = \frac{9}{32} f_{p0} \frac{A^2}{r_0^3} \qquad\qquad S_p = N_p \times 4\pi r_0^2 = \frac{9}{8}\pi \times f_{p0} \times \frac{A^2}{r_0} \tag{7}$$

respectively, where f_{p0} is the nanofiller volume fraction.

It is worth noting that, for the sake of simplicity, Eq. (7) has been derived by tacitly assuming a constant nanoparticle radius. Although in the previous literature nanoparticle radii distribution is described by a Galton distribution [9], it can be shown that even introducing such a distribution function in the analytical treatment, the number of nanoparticles subjected to debonding can be linked to the mean value of the radius, thought of as a deterministic value [14]. This corroborates the simplified analysis carried out herein.

4. Determination of the debonding strain energy density and debonding-induced toughness improvement

The energy produced at the nanoscale by debonding of a single nanoparticle is:

$$U_{db} = \gamma_{db} \times 4\pi r_0^2 \tag{8}$$

where γ_{db} is the interfacial energy. Accordingly, the strain energy density in a RVE (microscale) can be calculated as:

$$u_{db} = U_{db} \times \frac{3f_{p0}}{4\pi r_0^3} = \gamma_{db} \times 4\pi r_0^2 \times \frac{3f_{p0}}{4\pi r_0^3} = 3\frac{\gamma_{db}}{r_0} f_{p0} \tag{9}$$

Finally, the macroscale increment in terms of Strain Energy Release Rate can be estimated by [15, 16]:

$$\Delta G_{db} = 2 \times \int_0^{\rho^*(\phi=\pi/2)} u_{db} d\rho = 3\frac{\gamma_{db}}{r_0} f_{p0} A = 3 \times \frac{\gamma_{db}}{r_0} \times \frac{1}{(C_h)^2} \times \frac{2(1+\nu_o)^2 K_I^2}{9\pi\sigma_{cr}^2} \times f_{p0} \tag{10}$$

By further noting that $G = K_I^2 / E_o \times \left(1 - \nu_o^2\right)$, the toughness improvement due to debonding becomes:

$$\Delta G_{db} = \frac{2}{3\pi} \times \frac{\gamma_{db}}{r_0} \times \frac{1+\nu_o}{1-\nu_o} \times \frac{E_o}{\sigma_{cr}^2 (C_h)^2} \times f_{p0} \times G_c = f_{p0} \times \psi_{db} \times G_c \tag{11}$$

where now G_c is the fracture toughness of the nanocomposite.

Finally, assuming $G_c = G_m + \Delta G_{db}$, being G_m the matrix fracture toughness, the nanocomposite fracture toughness turns out to be:

$$G_c = \frac{G_m}{1 - f_{p0} \times \psi_{db}}$$ (12)

5. Example of application and discussion

Examples of application of the analytical results obtained in previous sections are shown in Figure 2. The bulk material properties match those of the epoxy resin used in [9].
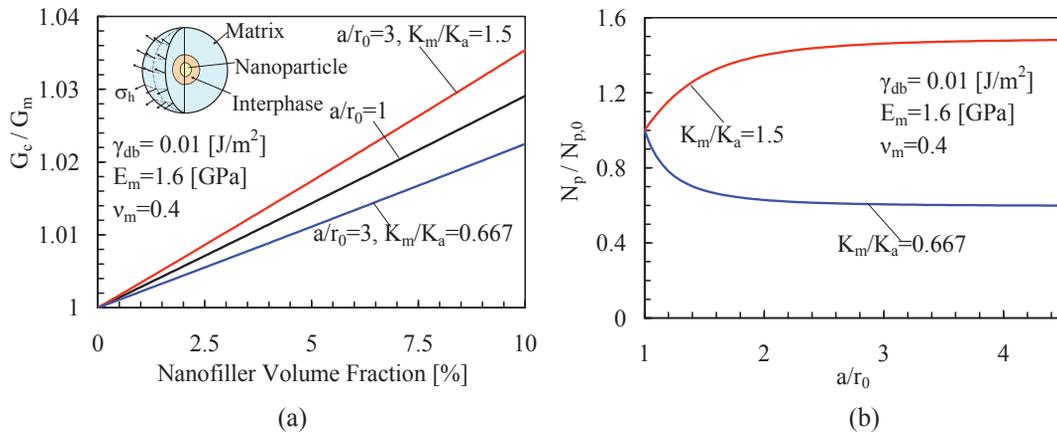
Fig. 2. (a) Toughness improvement according to Eq. (12) versus the nanofiller volume fraction (different interphase size and properties); (b) influence of the interphase size and properties on the number of debonded nanoparticles, N_p ($N_{p,0}$ represents the number of debonded particles neglecting the interphase). K_m and K_a are the matrix and the interphase bulk moduli, respectively. The bulk material properties match those of the epoxy resin used in [9].

In particular Fig. 2a shows the toughness improvement due to debonding versus the nanofiller volume fraction; three different interphase size and properties have been considered. It is evident that, in all cases, the improvement is rather limited (less than 5%). On the other hand, it is also quite easy to prove that debonding is a necessary condition for the subsequent plastic yielding around nanovoids created by debonded nanoparticles, such a toughening mechanism being of primary concern [11, 14]. With the aim to prove that, as a first approximation, we can substitute the linear elastic solution for the undebonded particle [12] within the Tresca yield condition. By so doing:

$$\sigma_{rr} - \sigma_{\theta\theta} = \sigma_n \times \frac{1 - 2\nu_a}{1 - \nu_a} > \sigma_{Ya}$$ (13)

where σ_{Ya} is the yield strength of the interphase. As soon as the interphase behaves plastically, ν_a becomes 0.5 and the yielding condition can never be satisfied. This suggests that nanoparticle debonding can be thought of as a "secondary toughening mechanism" being more important as a trigger for other induced mechanisms, like plastic yielding. A similar conclusion, without considering the influence of an interphase zone, was drawn by Williams [11].

To this end, it is extremely important to estimate the extension and the shape of the Debonding Region

(DBR) as well as the number of nanovoids created by debonding of nanoparticles, given by Eq. (6) and Eq. (7). Finally, Fig. 2b shows that the interphase size and properties have a great influence on the number of debonded nanoparticles, N_p. In more details the greater the K_m/K_a the larger N_p is. For the considered cases deviations are within $\pm 30\%$. This result is extremely important and proves that as different functionalizers lead to different elastic properties of the interphase, the number of voids, meant as sites of energy dissipation, is affected by surface treatments.

6. Conclusions

The work provides a multiscale model to assess the extension of the debonding region (DBR) and the toughness improvement due to nanoparticle debonding, considering a crack in the nanoparticle filled polymer. The model accounts for the effect of the size and the properties of an interphase embedding the nanoparticle and created by the inter and supra-molecular interactions arising at the nanoscale.

It has been proven that, even if nanoparticle debonding commonly results in a limited toughness improvement (less than 5% for all the analysed cases), it is a necessary condition for the subsequent plastic yielding around voids. This suggests that nanoparticle debonding can be thought of as a "secondary toughening mechanism" being more important as a trigger for other induced mechanisms, like plastic yielding. It has also been shown that the interphase size and properties have a great influence on the number of nanovoids created by debonded nanoparticles.

Acknowledgements

References

[1] Odegard GM, Clancy TC, Gates TS. Modeling of mechanical properties of nanoparticle/polymer composites. Polymer;**46**:553-62.

[2] Yu S, Yang S, Cho M. Multi-scale modeling of cross-linked epoxy nanocomposites. Polymer 2009;**50**:945-952.

[3] Scocchi G, Posocco P, Danani A, Pricl S, Fermeglia M. To the nanoscale and beyond! Multiscale molecular modeling of polymer-clay nanocomposites. Fluid Phase Equilib 2007;**261**:366-74.

[4] Fermeglia M, Pricl S. Multiscale modeling for polymer systems of industrial interest. Progress Org Coat 2007;**58**:187-99.

[5] Thostenson ET, Chou TW. On the elastic properties of carbon nanotube-based composites: modeling and characterization. J Phys D 2003;**36**;573–82.

[6] Luo JJ, Daniel IM. Characterization and modeling of mechanical behavior of polymer/clay nanocomposites. Compos Sci Technol 2003;**63**:1607–16.

[7] Wetzel B, Rosso P, Haupert F, Friedrich K. Epoxy nanocomposites – fracture and toughening mechanisms. Eng Fract Mech 2006;**73**:2375–98.

[8] Zhao S, Schadler LS, Duncan R, Hillborg H, Auletta T. Mechanisms leading to improved mechanical performance in nanoscale alumina filled epoxy. Compos Sci Technol 2008;**68**:2965–75.

[9] Chen JK, Huang ZP, Zhu J. Size effect of particles on the damage dissipation in nanocomposites. Compos Sci Technol 2007;**14**:2990–96.

[10] Lauke B. On the effect of particle size on fracture toughness of polymer composites. Compos Sci Technol 2008;**68**:3365–72.

[11] Williams JG. Particle toughening of polymers by plastic void growth. Compos Sci Technol 2010;**70**:885–91.

[12] Zappalorto M, Salviato M, Quareasimin M. Influence of the interphase zone on the nanoparticle debonding stress. Under review.

[13] Ajayan PM, Schadler LS, Braun PV. Nanocomposite science and technology. Wiley-VCH,2003, ISBN 3527303596.

[14] Zappalorto M, Salviato M, Quaresimin M. Toughening of nanocomposites by debonding and subsequent plastic yielding. Under preparation.

[15] Freund LB, Hutchinson JW. High-strain-rate crack growth in rate dependent plastic solids. J Mech Phys Solids 1985;**33**:169-91.

[16] Huang Y, Kinloch AJ. Modelling of the toughening mechanisms in rubber-modified epoxy polymers. Part II A quantitative description of the microstructure-fracture property relationships. J Mater Sci 1992;**27**:2763-69.